

The Kuril Tsunamis of November 15, 2006, and January 13, 2007: Two Trans-Pacific Events

Academician N. P. Laverov^a, Corresponding Member of the RAS L. I. Lobkovsky^b,
Corresponding Member of the RAS B. W. Levin^c, A. B. Rabinovich^b, E. A. Kulikov^b,
I. V. Fine^d, and R. E. Thomson^d

Received January 23, 2009

DOI: 10.1134/S1028334X09040333

On December 26, 2004, a catastrophic earthquake ($M_w = 9.3$) occurred near the northwestern coast of Sumatra Island in the Indian Ocean. The tsunami generated by this event caused unprecedented destruction (with more than 226 000 casualties) and was one of the worst natural disasters in human history [15]. Analysis of this event performed at the Institute of Oceanology, RAS immediately after this event, revealed firstly, that the source of the earthquake of December 26, 2004, was located in a large seismic gap region where strong earthquakes had not been observed for more than 150 years; and secondly, that a similar seismic gap is located in the central part of the Kuril Kamchatka Subduction Zone [1, 4].

The possibility that a catastrophic earthquake and associated tsunami could occur within this gap was estimated to be extremely high and, correspondingly, this region requires thorough study and permanent geophysical monitoring. To examine this seismic gap, the Russian Academy of Sciences carried out two geophysical expeditions onboard the R/V *Akademik Lavrentiev* in August and September 2005 and 2006. During these expeditions, the structure of the subduction zone in the region of the Central Kuril gap was studied in detail and the region of the expected earthquake was located more precisely. The results of the research expeditions were used for prognostic tsunami calculations under differ-

ent scenarios of a possible earthquake source [2, 5]. In 2006, a precise geodesic basis was developed to estimate the velocities of tectonic motions on the Kuril Islands and to determine coseismic effects needed for future geodynamic investigations in the conjunction zone between the Pacific and North American (Okhotsk) lithospheric plates. The arc of the Kuril Islands was instrumented with a network of GPS sensors along its entire extension. This network includes five permanent observational sites (on Shikotan, Kunashir, Iturup, Paramushir, and Urup islands) and six temporary observational sites (on Urup, Ketoi, Matua, Harimkotan, Paramushir, and Tanfilieva islands) [12].

On November 15, 2006, at 11:14 UTC, a strong earthquake occurred in the region of the Central Kuril Islands ($M_w = 8.3$) exactly where it had been predicted [6–8, 13]. The earthquake epicenter was located on the continental slope of the Kuril–Kamchatka Trench approximately 90 km southeast of Simushir Island. Two months later, on January 13, 2007, a second earthquake with similar magnitude ($M_w = 8.1$) to the 2006 earthquake occurred in the same region. The epicenter of the main shock was located on the oceanic side of the trench 100 km to the east of the epicenter of the first earthquake (Fig. 1a) [6, 7, 13]. Both earthquakes caused transoceanic tsunamis that were recorded over the entire Pacific basin including the coasts of Japan, Hawaii, Alaska, Canada, Peru, Chile, New Zealand, and the West Coast of the United States [7, 11, 13]. The first tsunami was stronger. It damaged several towns on the Pacific coast of the United States, with the severest damage in Crescent City (California) located in 6300 km from the earthquake epicenter [9].

The authors of [6, 7, 11] analyzed the properties of the Kuril tsunamis of 2006 and 2007 in the near-field zone, i.e., in the region of the Central Kuril Islands and North Japan. According to coastal tide gauge data, the maximum tsunami wave heights in 2006 were recorded at Malokurilsk on Shikotan Island (155 cm) and at the Japanese stations Urakawa (118.3 cm) and Hachinohe (106.3 cm). In 2007, significant tsunami waves were

^a Presidium of the Russian Academy of Sciences,
Leninskii pr. 14, Moscow, 119991 Russia

^b Shirshov Institute of Oceanology, Russian Academy
of Sciences, Nakhimovsky prospekt 36, Moscow,
117997 Russia

^c Institute of Marine Geology and Geophysics,
Far East Division, Russian Academy of Sciences,
ul. Nauki 1b, Yuzhno-Sakhalinsk, 693022 Russia

^d Department of Fisheries and Oceans, Institute
of Ocean Sciences, 9860 West Saanich Road, Sidney,
British Columbia, V8L 4B2 Canada;
e-mail: A.B.Rabinovich@gmail.com

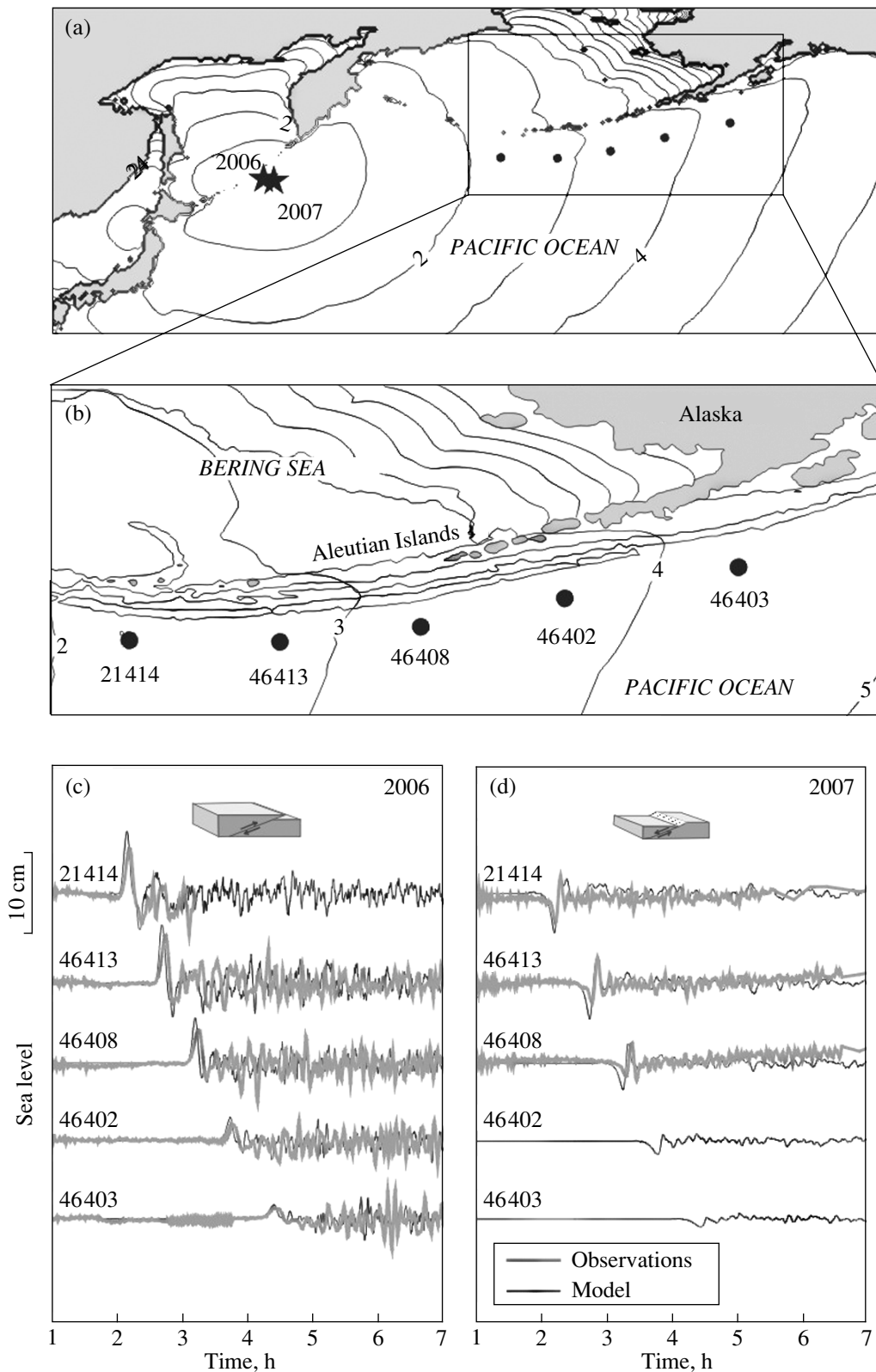


Fig. 1. Locations of the 2006 and 2007 earthquake epicenters and deep-ocean DART stations. (a) North Pacific; asterisks denote locations of the Kuril earthquake epicenters of November 15, 2006, and January 13, 2007; circles show the locations of bottom-mounted DART stations; thin solid lines show calculated isochrones (hours) of tsunami wave propagation in 2006 and 2007; (b) locations of five DART stations in the vicinity of the Aleutian Islands (United States); (c) tsunami observed at DART stations in 2006 and the results of their modeling; (d) the same for the tsunami in 2007. Mechanisms for the Kuril earthquakes in 2006 and 2007 are shown schematically in the upper parts of Figs. 1c and 1d.

also observed at these stations: 72, 35.3, and 29.1 cm, respectively. These stations were located at a distance of 500–700 km from the source. Unfortunately, no tide gauges were located in proximity to the source area (Central Kuril Islands); however, in the summer of 2007, several multidisciplinary field survey expeditions were organized in this region, which carried out detailed measurements of tsunami runup on the coasts of several islands [3]. The authors [3] believe that the maximum runup estimates of up to 17–20 m found on the coasts of Matua and Ketoy islands and the southeastern coast of Simushir Island are related to the tsunami of 2006. However, according to numerical calculations [11] based on the seismic models of the 2006 and 2007 earthquake sources

http://earthquake.usgs.gov/eqcenter/eqinthenews/2006/usvcam/finite_fault.php (a),

http://earthquake.usgs.gov/eqcenter/eqinthenews/2007/us2007xmae/finite_fault.php (b), the maximum runup of the second tsunami in the local zone near the sources should be even greater than the runup of the first tsunami (this fact is related to the local, small areal extent but large amplitude displacement in the central part of the 2007 earthquake source). According to GPS measurements for the earthquake of November 15, 2006, horizontal coseismic displacements were reliably determined at the permanent GPS stations on Iturup, Kunashir, Shikotan, Urup, and Paramushir islands. The maximum displacement (approximately equal to 60 mm) was recorded at the station on Urup Island. Horizontal coseismic displacements caused by the earthquake of January 13, 2007, were recorded at all permanent stations. The maximum value of approximately 18 mm was recorded at the permanent station on Paramushir Island. These values agree well with the seismic models used in [11].

In this work, we focus mainly on the far-field zone. It is worth noting that, despite the close location of the source zones and significant correlation between the two events (2006 and 2007), the differences between the second and first earthquakes are mainly in their seismic parameters. These differences were caused, first of all, by significant differences in their seismotectonic positions and by the consequent peculiarities of the destruction processes in the source regions. Although in both cases the rupture planes had similar orientations (parallel to the trench axis), the types of seismic motions under the island and oceanic slopes of the trench were diametric opposites. As a result, the first earthquake was of the upthrust type, while the second was of the normal fault type [6–8, 13]. The source area of the first earthquake was much larger (the aftershock zone of the earthquake occupied an area of $300 \times 220 \text{ km}^2$, whereas the area of the second one was $290 \times 90 \text{ km}^2$). Local “hot” zones of high intensity seismic motion were observed in the source region of the second earthquake [7, 8, 13]. Differences in the seismic source mechanisms led to significant differences in the parameters of the tsunami waves generated, in particu-

lar in the sign of the first oceanward propagating wave: it was positive for the tsunami of 2006 and negative for the tsunami of 2007. This peculiarity is clearly seen in Figs. 1c and 1d, in which records of the Kuril tsunamis of 2006 and 2007 obtained at deep-water DART¹ stations located in the region of the Aleutian Islands (locations of stations are shown in Fig. 1b) are shown together with the results of the corresponding model calculations. The tsunami measurements in the open ocean were not affected by any resonance peculiarities of the coastal topography, nonlinearity, refraction, or bottom friction. Therefore, they allow us to obtain an undisturbed tsunami signal, giving in this way important information about the physical properties of the tsunami source. At the same time, deep-water tsunami measurements play a particular role in the Tsunami Warning Service and are important for tuning and verification of tsunami propagation models [14].

Numerical simulations of the tsunamis of November 15, 2006, and January 13, 2007, were carried out for the entire Pacific Ocean using the model described in [7, 11] on the basis of the one-minute GEBCO depth dataset and actual source data. The results of Chen Ji were used to estimate the parameters of the 2006 and 2007 tsunami sources. Ji used a finite fault model to calculate displacements along the rupture plane for these earthquakes (a) and (b).

We subsequently used the well known Okada model [10], which allows us to recalculate seismic displacements into vertical deformations of the sea bottom. We solved the full Laplace equation to restore the initial ocean surface deviations. The application of the traditional long-wave model to restore the source could lead to significant errors, taking into account the fact that the extents of the deformation regions for the 2006 and 2007 earthquakes were comparatively confined [11]. However, we used the long-wave model in simulations of tsunami wave propagation.

Figures 1c and 1d provide examples of data from the 2006 and 2007 Kuril tsunami observations recorded at DART stations (Fig. 1b) and the results of numerical tsunami wave simulations for these stations. The calculated and observed wave parameters are presented in Table 1. During strong events, DART sensors automatically (or by an operator’s command) switch to alarm mode with data transmission every 15 s. Unfortunately, during the second event (2007) DART sensors 46402 and 46403 were switched off before the arrival of the tsunami wave. Therefore, data for the corresponding event are absent.

Generally, the results of the tsunami simulations and observations agree well. The model results describe correctly the general character of the oscillations, the time of the first wave arrivals, their sign (“±” in 2006

¹ DART is an acronym for Deep-ocean Assessment and Reporting of Tsunamis, a deep-water system of stations deployed by the United States along seismically active regions of the Pacific Ocean to monitor tsunami waves.

Table 1. Calculated and observed values for waves of the Kuril tsunamis of November 15, 2006, and January 13, 2007, for the region of the DART stations near the Aleutian Islands

DART stations	First semiwave				Second semiwave			
	amplitude, cm		travel time, h:min		amplitude, cm		travel time, h:min	
	observations	calculation	observations	calculation	observations	calculation	observations	calculation
Tsunami of November 15, 2006								
21414	+6.1	+7.6	2:11	2:09	-3.3	-4.5	2:23	2:20
46413	+6.0	+7.2	2:45	2:41	-2.6	-4.1	2:50	2:51
46408	+4.4	+5.5	3:15	3:11	-1.8	-1.8	3:22	3:17
46402	+2.1	+3.0	3:45	3:43	-1.1	-1.3	3:55	3:55
46403	+1.3	+1.5	4:23	4:23	-0.5	-0.5	4:36	4:35
Tsunami of January 13, 2007								
21414	-3.1	-6.9	2:13	2:12	+2.7	+2.5	2:18	2:17
46413	-2.8	-6.2	2:47	2:44	+3.0	+4.2	2:52	2:51
46408	-1.9	-4.6	3:18	3:15	+2.3	+3.5	3:24	3:20
46402	-	-2.3	-	3:47	-	+1.2	-	3:52
46403	-	-1.4	-	4:26	-	+0.3	-	4:32

and “±” in 2007), and the observed wave amplitudes (notable differences are seen only for the amplitude of the first semiwave of the 2007 tsunami). On the one hand, good correlation between the observations and calculations demonstrates the high quality of the numerical model; on the other hand, this is also evidence that the model accurately reproduced the initial parameters of the 2006 and 2007 tsunami sources, and consequently the seismic parameters of the earthquake sources.

The location of the DART stations in the direction of the wave propagation allows us to trace the evolution of the 2006 and 2007 tsunami waves with distance from the source. The 2006 tsunami wave arrived at the first DART station (21414) approximately two hours after the earthquake as a pronounced positive disturbance (sea level elevation) of approximately 6 cm. A slight level depression (-3.3 cm) followed. The entire period of this first wave was approximately 25 min; its trough-to-crest height was 9.4 cm. The same wave form was recorded at the next DART stations. The wave height gradually decreased with distance from the source: 8.6 cm (46413), 6.2 cm (46408), 3.2 cm (46402), and 1.8 cm (46403). The travel time of the wave from one DART station to another was approximately 30 min. It is clear that the form of the first wave was indicative of the dipole character of the seismic source with a depression on the inner (island) side and elevation on the outer (oceanic) side. A long tail of irregular oscillations with sufficiently smaller periods followed the first wave. The numerical model described this process quite well. The first oscillation was the strongest at the first three DART stations. However, at distant DART stations (46402 and 46403), the maximum waves were observed 1.5–2.0 h after the arrival of the first wave (Fig. 1c). It is likely

that the formation of these secondary maxima is related to the superposition of reflected and scattered tsunami waves.

In 2007, the evolution of the tsunami was approximately similar to that for the 2006 tsunami except that the first disturbance in 2007 was negative (-3.1 cm) and was followed by a positive semiwave with roughly the same amplitude (Fig. 1d). As noted previously, the opposite signs of the tsunami waves in 2006 and 2007 are related to the different seismic mechanisms of the associated earthquakes. The period of the first wave was 13–16 min. It was sufficiently shorter than the period of the 2006 tsunami, which is likely related to a significantly smaller transversal size of the source zone. It is noteworthy that the tsunami propagation time from the source to the DART stations for the two events was almost the same (with an accuracy of 2–3 min).

2006 tsunami waves propagating toward the east and southeast reached the Hawaiian Islands, Alaska, the western coasts of North and South America and New Zealand. Altogether, this tsunami was recorded by more than 200 digital coastal tide gauges, which provided a vast amount of data for further analysis. The results of thorough analysis of tide gauge records made by the authors demonstrated that tsunami waves with a height exceeding 1 m were observed in Japan (118 cm at Urakawa, Hokkaido Island, 140 cm at Miyakejima Island, and 101 cm at Chichijima Island), on the Hawaiian Islands (161 cm in Kahului and 119 cm in Haleiwa), on the North American coasts of Oregon (110 cm at Port Orford) and California (177 cm at Crescent City, 123 cm at Arena, 112 cm at Port San Luis), and in Mexico (128 cm at Ensenada). On the coasts of Peru, North Chile, and Easter Island, the maximum wave heights

Table 2. Statistical characteristics of the Kuril tsunamis based on measurements at individual coastal tide gauges in the Pacific

Station, region	Country	Coordinates*		November 15, 2006		January 13, 2007		Height ratio
		latitude	longitude	travel time, h:min	maximum height, cm	travel time, h:min	maximum height, cm	
Malokurilsk, Shikotan Island	Russia	43.850°	146.600°	1:08	155.0	1:09	72.0	2.15
Shemya, Aleutian Islands	United States	52.731	174.103	2:04	92.9	2:10	68.5	1.36
Miyakejima Island**	Japan	34.050	139.567	~2:25(?)	139.6	2:49	71.0	1.97
Chichijima Island	Japan	27.083	142.183	3:00	100.5	2:44	83.0	1.21
Midway Island	United States	28.207	-177.356	4:12	94.5	4:06	36.8	2.57
Kahalui, Hawaii	United States	20.898	-156.472	6:38	160.6	6:44	32.9	4.88
Crescent City, California	United States	41.745	-124.183	8:30	176.6	8:56	51.0	3.46
Easter Island	Chile	-27.150	-109.448	16:34	74.0	16:51	39.6	1.87
Santa Cruz, Galapagos Islands	Ecuador	-0.750	-90.317	17:38	66.2	18:09	26.4	2.51
Callao	Peru	-12.071	-77.174	20:05	72.8	20:33	30.4	2.39
Talkahuano	Chile	-36.683	-73.100	21:54	95.6	22:41	22.6	4.23
Timaru**	New Zealand	-44.392	171.254	18:49	58.0	~18:40(?)	17.0	3.41

* Positive latitude and longitude correspond to the Northern and Eastern hemispheres; Negative latitude and longitude correspond to the Southern and Western hemispheres.

** The exact times for the first tsunami arrival at Miyakejima (Japan) and second tsunami arrival at Timaru (New Zealand) are not well defined.

ranged from 75 cm to 1 m, and in New Zealand, from 30 to 60 cm. Thus, the Kuril tsunami of November 15, 2006, was the strongest transoceanic tsunami in the Pacific Ocean since 1964 (Alaska earthquake and tsunami). The number and quality of the records for this event are unrivaled [7, 11].

The earthquake of January 13, 2007 also generated a transoceanic tsunami but slightly weaker than the tsunami of 2006. Notable oscillations were recorded at a number of stations in the northern part of the Pacific Ocean: 83 cm at Chichijima Island (Japan), 71 cm at Miyakejima Island (Japan), 68.5 cm at Shemya Island (Aleutian Islands), 37 cm at Midway Island, and 51 cm at Crescent City and Arena on the Californian coast. Waves with a height of 40 cm were recorded on Easter Island in the southern part of the Pacific Ocean, 15–35 cm on the coast of northern Chile, and 15–20 cm in New Zealand. At most sites, the maximum wave heights occurred a significant time after the arrival of the first wave, as was the case after the earthquake of November 15, 2006.

Table 2 presents parameters of the observed tsunami waves at several typical stations located in different regions of the Pacific Ocean. The tsunami travel (propagation) times to these stations varied over a wide range: from one hour to 22–23 h. A good correlation between travel times for the two events was observed. An interesting regularity was found: travel times for

near-source stations coincided especially closely, while for distant stations the second tsunami was delayed by 20 to 45 min relative to the first. We assume that the latter effect is related to the influence of wave dispersion and to the parameters of the initial sources for the two events: the source of the second event was much smaller; hence, the generated waves had smaller lengths and higher frequencies (this is clearly seen by comparing Figs. 1c and 1d). Thus, they were subjected to a stronger retardation effect by wave dispersion.

The data presented in Table 2 and in Fig. 2b (constructed using all available stations) do not reveal any evident correlation between the heights of the recorded waves and distance from the source. For example, the 2006 tsunami waves in Northern California (approximate distance is 6500 km, travel time is 8–9 h) were stronger than in Japan (700–2500 km, 1.5–3 h). At several sites along the Chilean coast (~16 000 km, 22 h) the heights were greater than on Shemya Island (Aleutian Islands) (1640 km, 2 h). On the one hand, this could have been caused by the determining influence of the bottom and coastal topography on the intensity of the arriving tsunamis (these factors appear to be more important than the distance from the source); on the other hand, this observation demonstrates that tsunamis can be a serious threat even for remote inhabited locations at distances of 10 000–15 000 km from the source.

Figure 3 presents results from the numerical modeling of the 2006 and 2007 Kuril tsunamis for the Pacific basin and comparisons of model output with coastal tide gauge observations. It is evident that the general character of the energy propagation is similar for both events.

The main energy flux for both events was directed to the southeast toward the Hawaiian Islands and further to South America. The numerical results are in good agreement with observations. Submarine ridges (Emperor and Hawaiian) strongly influenced the propagation of the waves. These ridges caused diffraction and partial reflection of the waves resulting in the formation of individual wave trains and significant spatial and temporal variations in wave heights (see also [9, 13] where this problem was discussed). The individual “tongues” of energy propagation are confined to large features in the bottom topography, such as the Mendocino Fracture Zone. It is likely that this fracture facilitated focusing of the tsunami energy near the coast of North California leading to severe destruction in the port of Crescent City [9].

The results of numerical calculations demonstrate that the main energy of the 2006 tsunami wave propagated from the source region in a wide swath, while for the 2007 tsunami it propagated in a narrow beam similar to that from a lighthouse beacon. This is related to the properties of the associated source regions: the source region for the 2006 tsunami was of greater extent but the vertical displacements were more intense for the 2007 source (source parameters were estimated based on Ji’s models). According to the calculations [7, 11], the maximum heights of tsunami waves (H_{2006} and H_{2007}) occurred within the near-field zone, i.e., to the coast of the Central Kuril Islands (which agrees with the results of field measurements in this region [3]). The calculated tsunami wave heights for the events had similar values in the near-field zone, but the 2006 tsunami wave heights dominated strongly with increasing distance from the source. The coastal tide gauge data allow us to estimate the ratio between the observed heights of the two tsunamis.

As noted previously, instrumental measurements for these tsunamis were unfortunately absent in the near-field zone. The closest tide gauge to the sources (Malokurilsk) was located at a distance exceeding 600 km. As a consequence, the estimates in Fig. 2 are derived from stations located at distances of 600–16 500 km from the sources. On average, the tsunami height ratio $r = \frac{H_{2006}}{H_{2007}} \approx 2.5$. This ratio tends to increase with increasing distance from the source: $r(x) \approx 2.31 + 3.35 \times 10^{-5}x$, where x is the distance in km. The different frequency composition of the generated tsunami waves for the two events (lower frequencies for the 2006 tsunami and higher frequencies for the 2007 tsunami) led to different responses of the local basins to the arriving

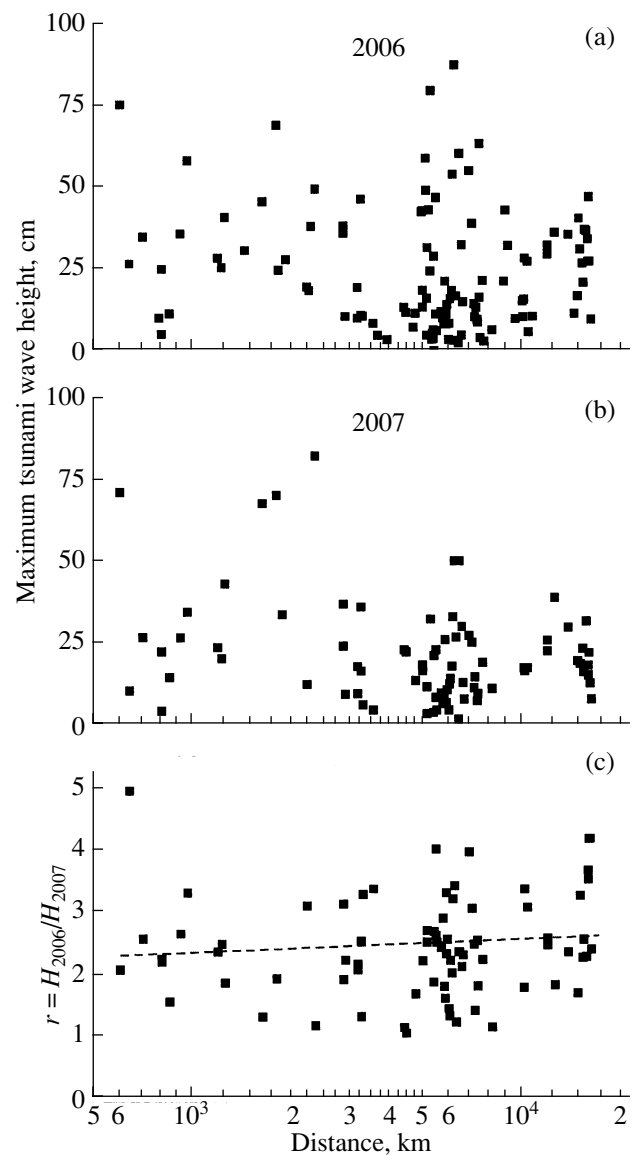


Fig. 2. Maximum observed tsunami wave heights in 2006 and 2007 versus the distance of the corresponding coastal tide gauges from the sources of the Kuril earthquakes and ratio of maximum tsunami heights in 2006 and 2007.

waves. Eventually, they caused significant scatter in the coefficient r (Fig. 2).

We note that, in general, the two major tsunamis caused by strong earthquakes near the coasts of the Central Kuril Islands yielded unique research material and that, once again, demonstrated the catastrophic potential for this region and the serious threat of the Kuril tsunamis for the entire basin of the Pacific Ocean. At the same time, analysis of the DART observations in the open ocean and comparison of these observations with the results of numerical modeling indicate that significant progress in all stages of tsunami research has been achieved in recent years, in particular, in the reconstruction of tsunami source mechanisms, in open-

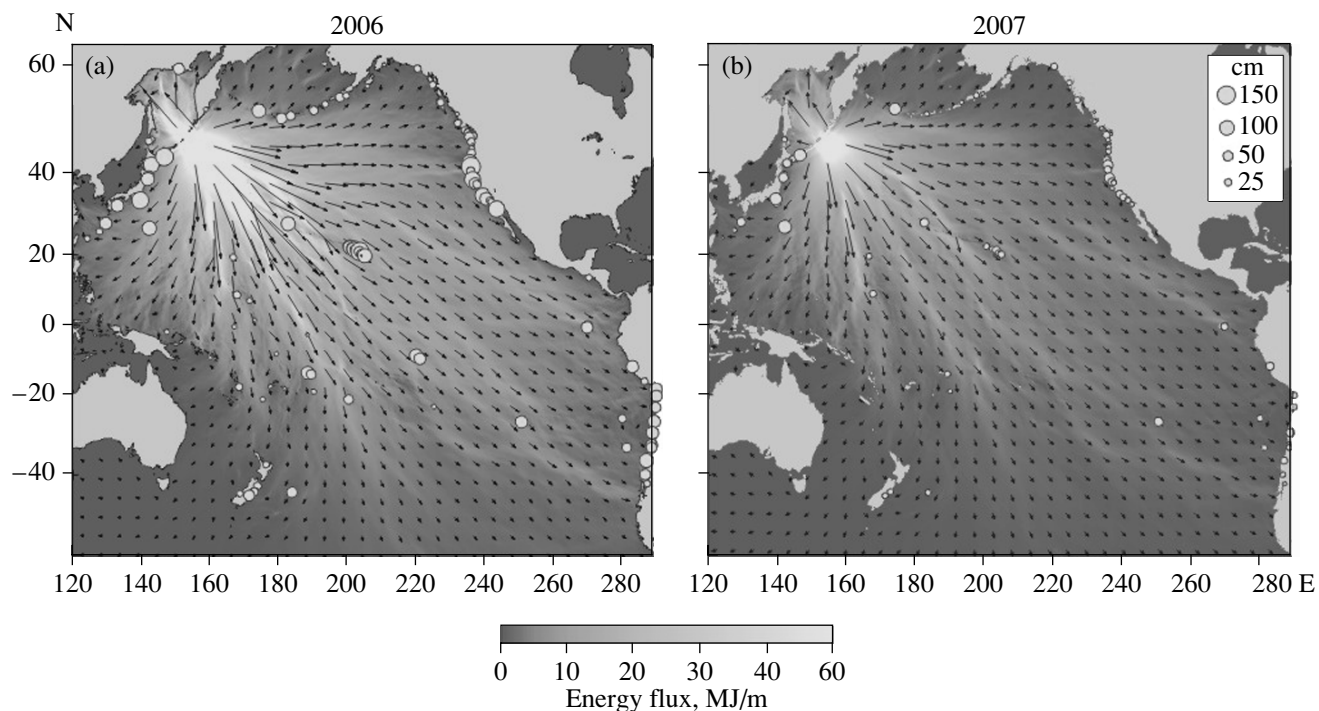


Fig. 3. Numerical simulations of the tsunami energy flux on (a) November 15, 2006, and (b) January 13, 2007, in the Pacific Ocean. Circles denote the observational sites for the corresponding tsunamis; the area of the circles is proportional to the square root of the observed tsunami wave heights.

ocean tsunami measurements, and in numerical modeling of tsunami waves.

ACKNOWLEDGMENTS

The authors thank many scientists and specialists from the United States, Canada, Japan, New Zealand, Chile, Australia, France, and Mexico who provided the data used in this research. This study was supported by the Russian Foundation for Basic Research (projects no. 08-05-00909 and 08-05-13582).

REFERENCES

1. N. P. Laverov, S. S. Lappo, L. I. Lobkovsky, and E. A. Kulikov, in *Fundamental Studies of Oceans and Seas*, Vol. 1 (Nauka, Moscow, 2006), pp. 191–209 [in Russian].
2. N. P. Laverov, S. S. Lappo, L. I. Lobkovsky, et al., *Dokl. Earth Sci.* **408**, 787 (2006) [*Doklady Ross. Akad. Nauk* **408**, 818 (2006)].
3. B. W. Levin, V. M. Kaistrenko, A. V. Rybin, et al., *Dokl. Earth Sci.* **419**, 335 (2008) [*Doklady Ross. Akad. Nauk* **419**, 188 (2008)].
4. L. I. Lobkovsky, *Vestnik RAEN*, No. 2, 53 (2005).
5. L. I. Lobkovsky, R. Kh. Mazova, L. Yu. Kataeva, and B. V. Baranov, *Dokl. Earth Sci.* **410**, 1156 (2006) [*Doklady Ross. Akad. Nauk* **410**, 528 (2006)].
6. L. I. Lobkovsky, E. A. Kulikov, A. B. Rabinovich, et al., *Dokl. Earth Sci.* **418**, 320 (2008) [*Doklady Ross. Akad. Nauk* **418**, 829 (2008)].
7. L. I. Lobkovsky, A. B. Rabinovich, E. A. Kulikov, et al., *Oceanology* **49** (2), (2009) [*Okeanologiya* **49** (2), (2009)].
8. Y. Fujii and K. Satake, *Bull. Seism. Soc. Amer.* **98** (3), 1559 (2008).
9. Z. Kowalik, J. Horillo, W. Knight, and T. Logan, *J. Geophys. Res.* **113** (1), C01020 (2008), doi: 10.1029/2007JC004402.
10. Y. Okada, *Bull. Seismol. Soc. Amer.* **75**, 1135 (1985).
11. A. B. Rabinovich, L. I. Lobkovsky, I. V. Fine, et al., *Adv. Geosci.* **14** (1), 105 (2008).
12. G. M. Steblov, M. G. Kogan, B. W. Levin, et al., *Eos Fall Meet. Suppl.* **88** (52) (2007), Abstract G13A–0916.
13. Y. Tanioka, Y. Hasegawa, and T. Kuwayama, *Adv. Geosci.* **14** (1), 129 (2008).
14. V. V. Titov, F. I. González, E. N. Bernard, et al., *Nat. Hazards* **35**, 41 (2005).
15. V. V. Titov, A. B. Rabinovich, H. Mofjeld, et al., *Science* **309** (1), 2045 (2005).